Surface & Coatings Technology 320 (2017) 349–356

Contents lists available at ScienceDirect

Surface & Coatings Technology

journal homepage: www.elsevier.com/locate/surfcoat

# Characterization of interfacial delamination in multi-layered integrated circuit packaging

Pamela Lin [a,b], Fei Shen [a], Alfred Yeo [a,b], Bo Liu [a], Ming Xue [b], Huan Xu [b], Kun Zhou [a,*]

[a] School of Mechanical and Aerospace Engineering, Nanyang Technological University, Singapore, 50 Nanyang Avenue, Singapore 639798, Singapore
[b] Infineon Technologies Pte Ltd, 8 Kallang Sector, Singapore 349282, Singapore

ARTICLE INFO

*Article history:*
Received 19 August 2016
Revised 21 November 2016
Accepted in revised form 15 December 2016
Available online 18 December 2016

*Keywords:*
Multi-layered system
Indentation
Delamination
Molecular dynamics simulation
Finite element method
Cohesive zone modeling

ABSTRACT

It is challenging to understand and predict interfacial delamination in multi-layered integrated circuit (IC) packaging due to the difficulties in experimentally quantifying the critical fracture energy of interfacial adhesion. This study takes a combined approach based on molecular dynamics (MD) simulation and finite element method (FEM) to characterize the interfacial fracture energy and predict delamination in the Cu/Ti/$SiO_2$/Si multilayer systems. MD simulation is first conducted on each interface of the multiple layers at the atomistic level to obtain the material parameters such as the critical interfacial fracture energy that are required for the interfacial cohesive constitutive relation. Then, FEM is used to model and predict the interfacial delamination of the multi-layered system under indentation loading at the macroscale with the cohesive zone being considered around the delamination or crack tips. Finally, the indentation damage test is performed to validate the modeling results. The proposed combined modeling approach will have the potential to provide guidance in design and applications of IC packaging for improved stability and reliability.

© 2016 Elsevier B.V. All rights reserved.

## 1. Introduction

In the recent years, the mechanical robustness and reliability of three-dimensional (3D) integrated circuit (IC) packaging has become tremendously challenging due to its continuous reduction in size and increase in vertical integration [1]. Thermal problems such as cracking in the oxide layers and interfacial delamination are increasingly dominant due to the presence of high heat density in the small system size. Furthermore, the mismatch in the coefficients of thermal expansion between dissimilar materials induces thermomechanical stresses, leading to problems such as thermal warpage and eventually resulting in interfacial delamination failure.

Interfacial delamination is initiated by the nucleation of a crack at the interface or near the interface, which will then propagate when the stresses are sufficiently high and result in a catastrophic failure of the IC packaging [2]. The interfacial fracture energy, also known as the practical work of adhesion, is an essential property for the performance and reliability of the 3D ICs as it determines the amount of energy needed for delamination to occur. This property accounts for the thermodynamic work of adhesion between the interface and the energy dissipated by the materials probably due to plastic deformation and other inelastic contributions [3]. Thus, interfacial delamination failure is not only dependent on the mechanical properties of the layers, such as adhesion strength, reactivity and surface roughness but also the chemical and bonding characteristics at the interface and the stress distribution generated by external loading during the assembly and operating processes. There, an accurate failure prediction of interfaces cannot be made unless these material properties are well-considered [4].

The characterization of such interfacial fracture energies between the interlayers is an important but yet inadequately resolved problem. This problem is further exacerbated in the 3D ICs whereby the increase in vertical integration and reduction in size have resulted in the introduction of new material layers and high density interconnection. Many works have employed conventional numerical and experimental approaches such as, linear elastic fracture mechanics (LEFM), finite element modeling (FEM), four-point bend test, blister test, scratch test, indentation test and laser spallation technique, to analyze and characterize the interfacial delamination failure [5–11]. LEFM calculates the critical stress intensity factors and energy release rates at the crack tip as singular and infinite, which is physically unrealistic. Furthermore, as plastic deformation at the interface occurs before fracture, LEFM alone is inadequate to characterize delamination failure.

On the other hand, FEM based on the cohesive zone modeling (CZM) uses the critical interfacial energies of different interlayers as the governing criterion for failure and is commonly used to solve fracture mechanics problems at the macroscale [12]. During thermomechanical loading, the interface behaves like a nonlinear material, undergoing damage initiation and delamination propagation which can be

* Corresponding author.
*E-mail address:* kzhou@ntu.edu.sg (K. Zhou).

http://dx.doi.org/10.1016/j.surfcoat.2016.12.050
0257-8972/© 2016 Elsevier B.V. All rights reserved.

described by a nonlinear traction-separation law based on CZM. The material parameters required to be input into the traction-separation law are usually experimentally derived.

Experimentally, the scratch test measures the force and displacement of the scratch tip to generate an interfacial crack and spalling, while the indentation test can be used to either induce spontaneous buckling of the film or create indentation blisters to drive delamination. In the event of a crack in the material, such as thin-film or substrate cracking, the corresponding load-displacement (*P-d*) curves would indicate a reduction in the stiffness. Subsequently, this will cause a change in the area under the *P-d* curve which corresponds to the work done for creak initiation. Such discontinuities are usually dependent on the failure mechanisms which may vary for different test systems. However, there is no evidence whether interfacial cracking will give rise to any discontinuities to the *P-d* curve [13,14].

Furthermore, when the system size approaches the nanoscale, it becomes more challenging to determine the interfacial properties accurately. A comprehensive and accurate description of the fracture at the interface cannot be provided based solely on the experimental or numerical approaches. The lack of knowledge in understanding of interfacial fracture has impeded 3D ICs design and technological advancement. Therefore, more viable methodologies are required to fully characterize the interfaces and predict interfacial delamination, so that the stability and reliability of the 3D multi-layered IC packaging can be improved.

One of such methodologies was developed by Namilae and Chandra [15] whereby a hierarchical multiscale model was used to study the mechanics of interfaces in carbon nanotube-based composites. This model used molecular dynamics (MD) simulation to derive the atomistic information of the interface and linked it to the macroscopic scale via the cohesive zone traction-displacement relations. Fan and Yuen [16] also used the same model to bridge the gap between the atomic and continuum levels. Similarly, the constitutive relations derived from MD simulation at the atomic level, in the form of traction-displacement curve, were incorporated into the CZM in FEM to investigate the interfacial fracture behavior at the continuum level. Subsequently, the corresponding failure force varying with the applied displacement was extracted from the simulated model and found to be in good agreement with the experimental data.

This study adopts a similar approach to characterize the interfacial fracture energy and predict interfacial delamination in the Cu/Ti/$SiO_2$/Si multi-layered system via MD and CZM-FEM simulations. Such a system is chosen as it is a common multi-layered structure found in the 3D ICs whereby the Si substrate is first coated with a dielectric layer which is then coated by thin intermetallic layers. This simple and yet effective approach is capable of bridging the microscopic and macroscopic structures by deriving the necessary CZM parameters from the MD simulation, to model the interfacial behavior when subjected to indentation loading, and subsequently to quantify the interfacial fracture energy at the macroscale accurately. Lastly, the FEM model is validated with experimental findings from the indentation damage test which allows cracking to happen in a controllable manner and is capable of measuring very small and localized deformation in the nano to micron range [17–19].

From this approach, the atomic behavior at the interface can be transferred to the continuum model so that interfacial delamination in 3D ICs packaging under different operating conditions can be predicted. Henceforth, experiments that are usually time-consuming and challenging are no longer required. Ultimately, the crack behaviors and the interfacial properties can be better understood and characterized. This study will be helpful to lay foundation to the knowledge of fracture mechanisms involved in the multi-layered IC devices and essential for materials selection and process control so as to improve the reliability of 3D IC packaging.

## 2. Methodologies

MD simulation serves as an excellent tool for modeling the interfacial properties at the atomistic level [20–23], as it is able to account for the bonding characteristics at the interface and the stress distribution generated by an applied load. With recent technological advancement and increase in computational power, this tool has been widely employed to investigate the failure mechanisms such as fracture and dislocations for a vast variety of materials [24,25]. In this study, MD simulation is performed to extract the interfacial properties in the Cu/Ti/$SiO_2$/Si multi-layered system to provide the cohesive parameters needed for FEM simulation.

Fig. 1 shows the computation cell of the Cu/Ti bi-layer system which has a dimension of 120 × 120 × 200 Å. The interface is assumed to be smooth with no surface roughness. A similar configuration is also adopted for the $SiO_2$/Si bi-layer system. Due to the lack of suitable interatomic potential to model the atomic interactions at the Ti/$SiO_2$ interface, MD simulation is not conducted for the Ti/$SiO_2$ bi-layer system and its interfacial properties is adopted from the literature [26]. The interactions among the Si-Si and Si-O atomic pairs are described by the Tersoff potential [27], and those among the Ti-Cu, Ti-Ti and Cu-Cu atomic pairs are described by the MEAM potentials [28,29]. Periodic boundary conditions are applied in the *x*- and *y*-directions, while free boundary condition is used along the *z*-direction to model a large-sized thin film. The simulation is conducted using the large-scale atomic/molecular massively parallel simulator (LAMMPS) [30].

Each material layer in the bi-layer system is initially relaxed to obtain the state with the minimum local potential energy. Afterwards, each layer is equilibrated at constant 300 K and zero external stress by using the constant pressure and temperature (NPT) ensemble via the Noose-Hoover thermostat for about 40 ps. Upon achieving equilibration, the system is then switched to the constant volume and temperature (NVT) ensemble. The structural information for each layer is then imported into a new simulation model to construct the bi-layer system as shown in Fig. 1.

In the new simulation model, the two layers are combined together with a separation distance of 10 Å. Such a large separation distance is chosen to allow ample time for the atoms at the periodic boundaries to rearrange themselves without the influence of the atoms from the other layer. Subsequently, the two layers are moved towards each other in steps of 0.05 Å followed by the relaxation of 0.5 ps until they are ~3 Å distance apart. At the short separation distance of ~3 Å, the bi-layer system will relax under the NVT ensemble for 10 ps to allow the interfacial bonds to form and to attain a globally stabilized structure. Subsequently, as high-stress sites at the interface may be present due to the formation of new interfacial bonds and the lattice mismatch between the two layers, energy minimization is then performed to ensure that local minimum energy state at the interface is obtained.

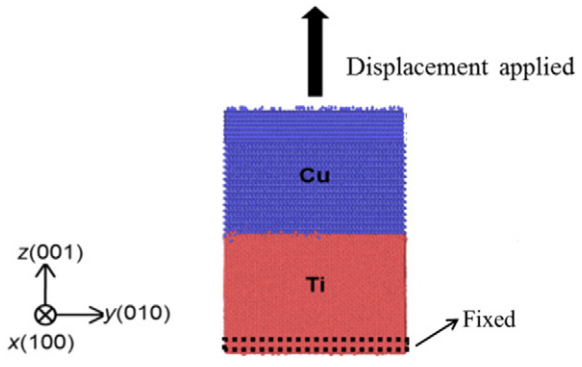


**Fig. 1.** Computational cells of the Cu/Ti system.

Upon the realization of the equilibrated structure, the tensile loading is applied by first fixing two layers of atoms, each with a thickness of ~10 Å, at the top and bottom of the system, respectively, and then displacing the top fixed layer along the *z*-direction at each simulation step. The deformation process is conducted at a strain rate of 0.002 $ps^{-1}$ until fracture occurs. The corresponding interfacial stress-strain relations are then obtained, whereby the interfacial stresses are computed using the virial theorem [21]. The effect of the strain rate is not taken into account in this study as its effect on the thermodynamic work of adhesion is negligible.

Due to the high computational cost, it is inefficient and not suitable to build a full MD model of the real geometry of nano/microelectronic IC packaging which is usually in hundreds nanometers or several micrometers. Hence, FEM is employed to bridge between the different length and time scales by transferring the information from the atomic level to the continuum level to obtain a good description of the interfacial fracture behavior at the macroscale.

At the continuum level, the CZM has been widely used to study the interfacial fracture process as it can avoid stress singularity at the crack-tip and represent the physics of the fracture process at the atomic scale [31–33]. When an external force is applied to a bilayer model, the upper and lower surfaces of the interface undergo separation. After a critical separation distance between these surfaces is attained, the interfacial crack will propagate. As such, energy flows into the fracture process zone for surface separation and therefore, the interfacial cohesive relation can be governed by the traction-separation law. This law is well described by the maximum cohesive stresses, the maximum separation of the interface and the interfacial fracture energy [34]. The advantage of using the traction-separation law is to eliminate the assumption that the interface is either fully-bonded, fully-debonded, or precracked. Since the interface crack nucleation and propagation criteria are inherently included in the traction-separation law, its onset and propagation can be captured and predicted.

Therefore, instead of using the conventional approach whereby the cohesive parameters are extracted from experiment, these parameters are derived from MD simulation as the MD model is able to provide the interfacial behavior of atoms at a localized area and also take into account the bonding and debonding at the interface. Subsequently, these MD parameters are input into the CZM to study the interfacial delamination response under external loading at the macroscale. Henceforth, the interface atomistic behavior governed by the interaction of atoms can be incorporated into the interface model in FEM and the potentials of the available simulation tools can be maximized.

In this study, the commercial nonlinear FEM software package ABAQUS is employed to simulate the delamination failure during the indentation testing of the Cu/Ti/$SiO_2$/Si multi-layered system. According to the geometric and loading configurations of the testing, the axisymmetric modeling is used in a quasistatic way without considering the time effect, as shown in Fig. 2. The 50 μm-diameter sphero-conical diamond tip indenter is modeled as a rigid body, and thus its deformation is ignored. The system beneath the indenter is divided into four substructures, namely the 1 μm-thick Cu layer, 60 nm-thick Ti layer, 1 μm-thick $SiO_2$ layer and 20 μm-thick Si, of which two adjacent layers are separated by a 1 nm-thick interface. The length of the system along the *x*-direction is 50 μm, which is about 10 times the half contact length for contact between the indenter and system.

All the individual material layers are modeled as isotropic elastic-plastic materials and the stress-strain data for these four materials are obtained from literature [35–37]. The interfaces are modeled using cohesive elements whose constitutive relation is governed by the bilinear traction-separation law (see Fig. 3) [38]. For each interface, the maximum nominal stress criterion is used to define the onset of the damage, and its evolution is described by the energy

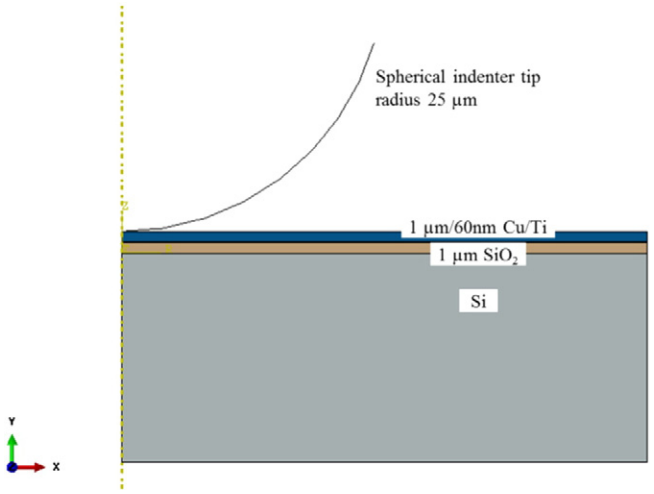


**Fig. 2.** Initial configuration of the FEM model of the Cu/Ti/$SiO_2$/Si system

evolution law:

$$\max\left\{\frac{\sigma_n}{\sigma_n^0}, \frac{\sigma_s}{\sigma_s^0}, \frac{\sigma_t}{\sigma_s^0}\right\} = 1 \tag{1}$$

$$\left\{\frac{G_n}{G_n^C}\right\}^{\alpha} + \left\{\frac{G_s}{G_s^C}\right\}^{\alpha} + \left\{\frac{G_t}{G_t^C}\right\}^{\alpha} = 1 \tag{2}$$

where $\sigma_n^0$, $\sigma_s^0$ and $\sigma_t^0$ represent the peak values of the nominal stress when the deformations are purely normal to the interface, in the first shear direction and the second shear direction, respectively; $G_n^C$, $G_s^C$ and $G_t^C$ refer to the critical fracture energies required to cause failure in the normal, the first, and the second shear direction, respectively. In this study, the mechanical behaviors in the two shear directions are assumed to be same as the normal behavior for the interfaces [39] and the Poisson's ratio of $\nu = 0.03$ is adopted for all the interfaces. The essential parameters required for the FEM simulations are the $\sigma_n^0$, $G_n^C$ and the initial stiffness $K_0$, which can be derived from the results of the abovementioned MD simulations, as listed in Table 1.

The 4-node axisymmetric elements, CAX4 and COHAX4, are used for the substructures and interfaces respectively. The regional meshing method is used for the modal meshing whereby the meshing refine quality is controlled and the transition from the contact area to the

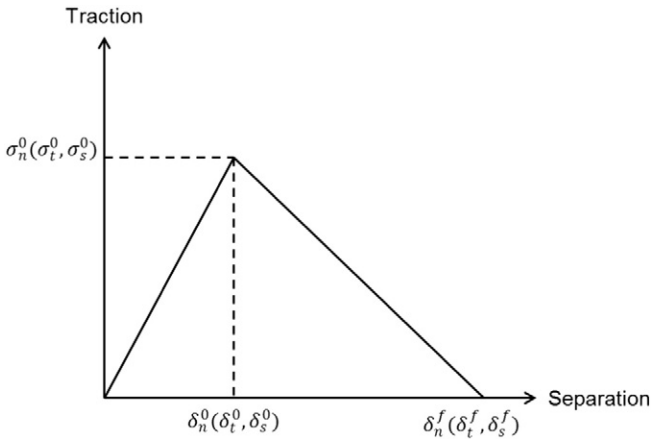


**Fig. 3.** Bilinear constitutive model used to represent the cohesive elements at the interfaces.

**Table 1**
Cohesive parameters obtained from MD simulation.

| Interfaces | $\sigma_{max}$ (GPa) | $D_{max}$ (nm) | $G$ (J/m$^2$) | Stiffness ($10^{10}$ MPa/mm) | $W$ (J/m$^2$) |
|---|---|---|---|---|---|
| Cu/Ti | 8.16 | 0.776 | 3.09 | 1.07 | 59.2 |
| Ti/$SiO_2$ [26] | 1.7 | 1.18 | 1 | 0.193 | – |
| $SiO_2$/Si | 16.9 | 3.35 | 29 | 0.546 | 7.25 |

far-field area is smoothened out. The mesh size in the contact zone is about 40 μm and the mesh convergence study is conducted at the start of the simulation. The friction force between the indenter and Cu/Ti/$SiO_2$/Si system is not considered here and small sliding conditions are adopted. The vertical motion of the bottom surface is constrained. The maximum vertical displacement of 2 μm, a value taken in experiment, is applied on the reference point of the indenter. The pre-existing cracks in the thin film and substrate and the residual stress in the thin film are also not considered for simplicity.

Lastly, the indentation damage test is conducted to provide validation to the interfacial fracture energy predicted by the CZM-FEM model. The multi-layered sample is prepared using the standard wafer fabrication process on a 100 mm-diameter wafer. The 1 μm-thick $SiO_2$ dielectric layer is first deposited onto the 500 μm-thick Si wafer via the plasma-enhanced chemical vapour deposition. Then, the 1 μm-thick Cu/Ti metallization layers are sputtered onto the $SiO_2$ dielectric layer. Lastly, the wafer is diced into a small die size of dimension 10 × 10 mm for experimental analysis.

The indentation damage experiments are carried out at ambient temperature using the microindentation system integrated with an acoustic emission (AE) sensor. The indentation process is performed using a 50 μm-diameter spherical diamond tip indenter and the *P-d* response and the AE signal are recorded simultaneously. When a crack event occurs, an ultrasonic wave will be emitted and detected by the AE sensor and consequently be reflected as a spike in the output voltage. Subsequently, the first AE signal detection will prompt the system to stop the loading process and the unloading process will ensue.

After the indentation test, the samples are placed under the focused-ion beam (FIB) to reveal the cross-sectional microstructure of the multi-layered structure at the indented region. Subsequently, the scanning electron microscopy (SEM) is used to provide insights to the cause of the AE signals and also conduct measurement of the delamination crack length for the quantification of the interfacial energy.

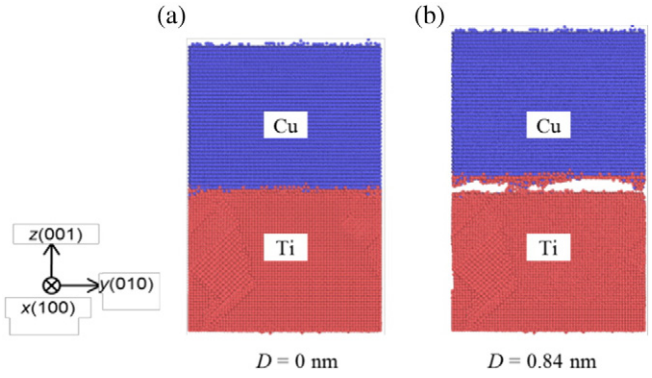


**Fig. 5.** The atomic configurations of the Cu/Ti systems under tensile loading at the separation distance $D$ of (a) 0 and (b) 2.79 nm.

## 3. Results and discussion

### 3.1. Simulation

The cohesive traction-separation relations obtained for each bi-layer system subjected to tensile loading in the *z*-direction at 300 K via MD simulation are shown in Fig. 4. The strain is applied incrementally, till the stress exceeds the critical value. At this critical stress, the atomic bonds are broken and fracture occurs. The maximum cohesive traction $\sigma_{max}$, the maximum separation distance $D_{max}$ and fracture energy $G$ can be obtained from the curves. The thermodynamic work of adhesion $W$ of each bi-layer can be calculated from $W = (E_A + E_B - E_{AB})/A$ where $E_A$, $E_B$and $E_{AB}$ are the total energies of the first material layer, second material layer and the combined bi-layer system, respectively, and $A$ is the interfacial area [40]. All the parameters computed via the MD simulation are summarized in Table I.

Theoretically, the fracture energy $G$ includes the thermodynamic work of adhesion $W$ and the energy dissipated by the materials due to plastic deformation and other inelastic contributions, and thus the value of $G$ should be larger than $W$. However, it is observed that the $G$

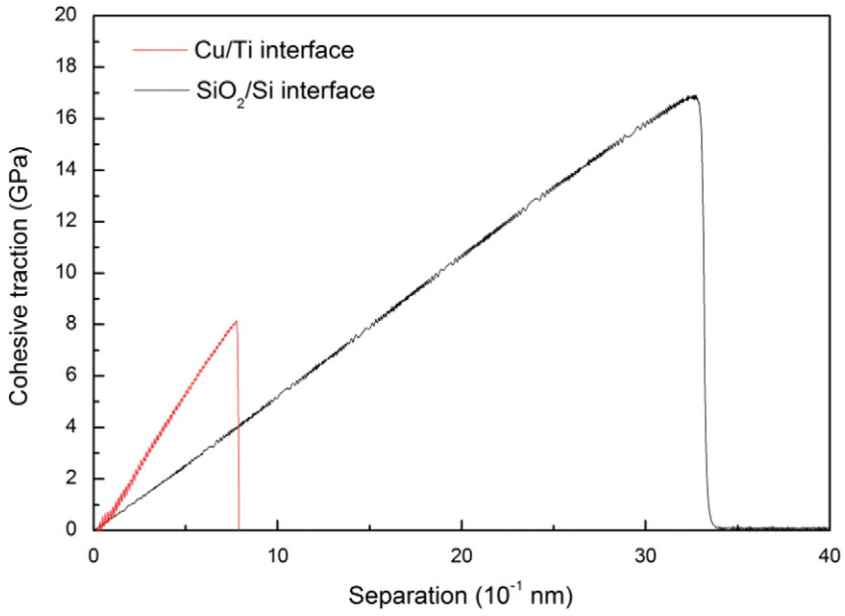


**Fig. 4.** Cohesive traction-separation relations of the Ti/Cu and $SiO_2$/Si systems under tensile loading at 300 K.

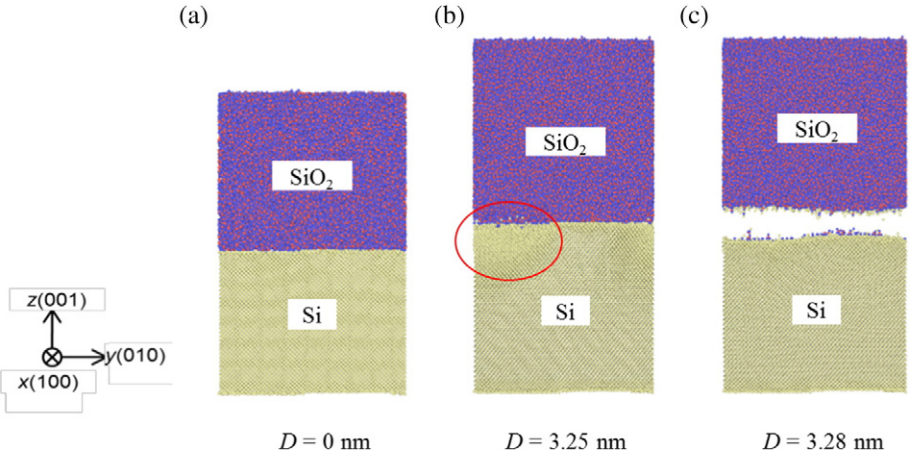


**Fig. 6.** The atomic configurations of the $SiO_2$/Si systems under tensile loading at $D$ of (a) 0, (b) 3.25 and (c) 3.28 nm.

for the Cu/Ti system (3.09 J/m$^2$) is significantly lower than its $W$ (59.2 J/m$^2$) (see Table 1). This is because the Cu and Ti layers are very well adhered, and thus when the tensile loading is applied, fracture did not happen exactly at the interface but an atomic layer away from the interface (Fig. 5b). Hence, this indicates that the Ti-Cu interfacial bonds are not broken and therefore the $G$ calculated is lower than the $W$. Nevertheless, this interfacial fracture energy obtained is realistic as the experimentally derived $G$ for the Cu/TiW system is ~1.5–2.5 J/m$^2$ [41]. The experimentally derived $G$ is slightly lower than that of the simulated value as the interface in the real system has certain surface roughness and may contain interfacial defects or impurities.

For the $SiO_2$/Si system, its $G$ (29 J/m$^2$) is significantly larger than its $W$ (7.25 J/m$^2$). This is expected as interfacial fracture occurs at the $SiO_2$/Si interface and large plastic deformation is observed before fracture, as shown in Fig. 6b and c. The $W$ obtained is in good agreement with the experimentally measured fracture energy of W/$SiO_2$/Si system which is ~5.5–9.0 J/m$^2$ [6]. Subsequently, these cohesive parameters derived from MD simulation are used to describe the cohesive traction-separation relation for the indentation damage model in FEM and this relation is assumed to be bilinear. The $W$ will be used as the fracture criterion in the CZM as it is independent of the system geometry and applied strain rate.

The indentation damage simulation is then performed and the deformation evolution process is illustrated in Fig. 7. At the indentation depth of 725 nm, it is observed that some of the cohesive elements have been removed, which indicates that the completion of the damage evolution process, and therefore the occurrence of the interfacial delamination. The delamination length $a$ obtained from the FEM is measured to be ~9.57 μm. Fig. 8 shows the $P$-$d$ curve and its corresponding damage dissipation energy graph of the Cu/Ti/$SiO_2$/Si system obtained from the CZM-FEM simulation. During the indentation loading, the external work done by the indenter is equal to the internal energy of the system which consists of namely the plastic energy dissipation, the stored elastic strain energy and the energy released when damage occurs, i.e. damage dissipation energy. Since the only failure mechanism observed in the indentation damage model is the delamination failure at the $SiO_2$/Si interface (Fig. 7), the energy released due to the damage will be used to drive the interfacial crack.

However, it is noted that there is no apparent discontinuity observed in the $P$-$d$ curve despite the occurrence of the damage. This is most probably due to the fact that the damage dissipation energy due to the delamination failure is of a very small magnitude of ~2.67 μJ (Fig. 8b). Hence, the damage energy loss is not apparently reflected in the $P$-$d$ curve. Most of the work done by the indenter is converted to plastic energy dissipation in the bulk Si substrate and stored elastic strain energy in the system. Thus, from the $a$ and damage dissipation energy, the $G$ can be calculated to be ~8.23 J/m$^2$.

### 3.2. Experimental validation

Fig. 9 shows the time history graph and the corresponding $P$-$d$ curve of a particular indent on the Cu/Ti/$SiO_2$/Si sample under indentation loading. During the loading process, the AE signal is first detected at the indentation depth of 2000 nm which also corresponds to the first 'pop-in' as shown in Fig. 9b. This is because when the sample is subjected to indentation loading, localized mechanical deformation and stresses are introduced in the thin films and substrate, resulting in the elastic-plastic deformation.

As the loading increases, high in-plane stresses are also induced along the interface and dislocations are emitted in the Si substrate. Subsequently, the interaction of the high-density dislocation formation may result in the substrate cracks as observed in Fig. 10b [42]. Stresses are released as the dislocation formation are emitted and this attributes to the 'pop-in' observed in the $P$-$d$ curve whereby there is no significant

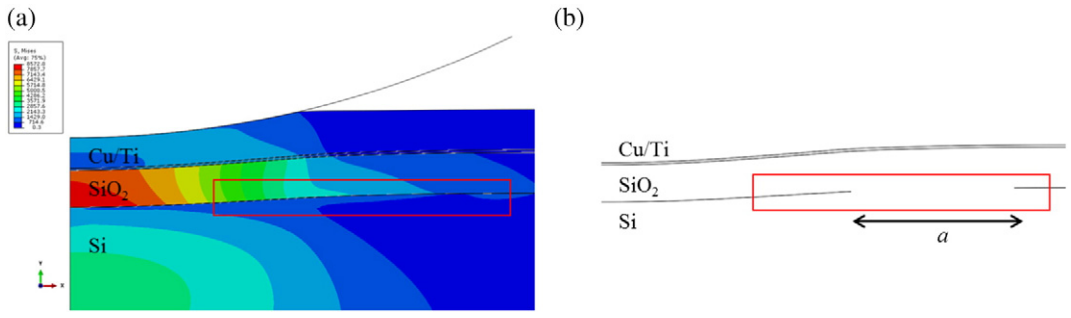


**Fig. 7.** (a) The von Mises stress distribution and (b) the corresponding damage state of the deformed model at the indentation depth of 725 nm. The onset of damage indicated by the removal of the cohesive elements is outlined in red.

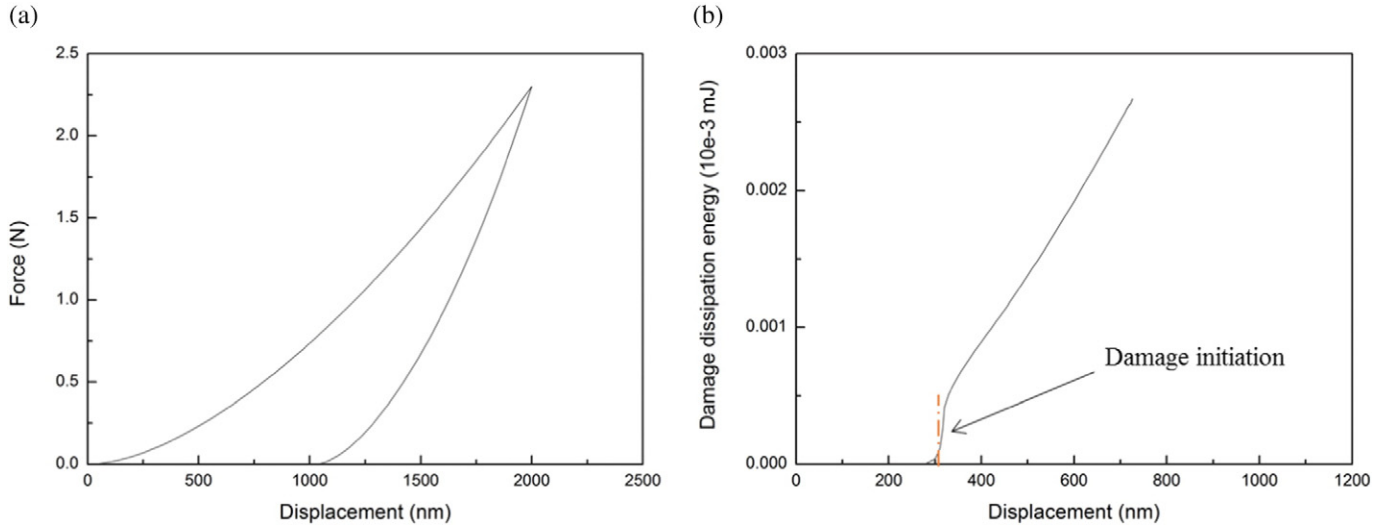


**Fig. 8.** (a) The *P-d* curve of the Cu/Ti/$SiO_2$/Si system and (b) the corresponding damage dissipation energy graph obtained from the FEM simulation.

increase in the loading force despite an increase in the indentation depth. Similarly, the formation of such cracks will also emit an ultrasonic wave which is then detected by the AE sensor and result in a spike in the voltage output (Fig. 9a).

After the first AE signal is detected, the system undergoes the unloading process. No discontinuities in the unloading curve are observed. During this process, the indented region of the Si substrate that is plastically deformed can no longer undergo complete elastic recovery. On the other hand, the thin-film layers around the indented region are able to experience greater elastic recovery as compared to the Si substrate due to their lower stiffness. As a result of this difference, localized tensile stresses and high stress concentrations are induced at the interface and near the edge of the indenter, respectively, and these stresses increase as the indenter retracts.

The FIB cut along the cross-section of the indented region in the post indentation analysis (Fig. 10b) shows that one of the substrate cracks formed during the loading process has propagated to the interface boundary. The presence of this crack near the interface boundary will result in high stress concentration at that region, leading to a significant increase in the localized tensile stresses. Subsequently, when the stored elastic energy in the deformed thin-film layers is released during unloading process, the interfacial adhesion strength between the $SiO_2$/Si layers can be easily overcome and the crack will propagate along the weak interface instead of penetrating through the $SiO_2$ thin film, resulting in the interfacial crack.

When the system reaches equilibrium, the interfacial crack propagation will eventually stop. This is evident in Fig. 10b whereby the interfacial crack is observed to be initiated from the substrate crack at 8.76 μm away from the center of indentation and propagated for a distance of 2.02 μm. This failure mode is similar to that of the constrained blister test whereby an annular delaminated region is observed. At the end of the unloading process, the second AE signal is detected. This signal is detected in all the indents regardless of the presence of an interfacial crack, and thus it is most likely to be attributed by the removal of the indenter from the surface of the sample. Neither the AE sensor nor the *P-d* output curve is able to provide any insights to the onset of interfacial delamination.

The work of interfacial fracture $G_c^i$ can be estimated from the fracture mechanics analysis model proposed by Wan and Dillard [43], which was derived based on the linear elasticity and energy balance approach. In the model, a circular thin film without initial residual stresses is fixed at its circumference and adhered to a cylindrical indenter that has the same diameter as the film. When the indenter is pulled up, a membrane stress is induced in the film and the indenter-film interface undergoes

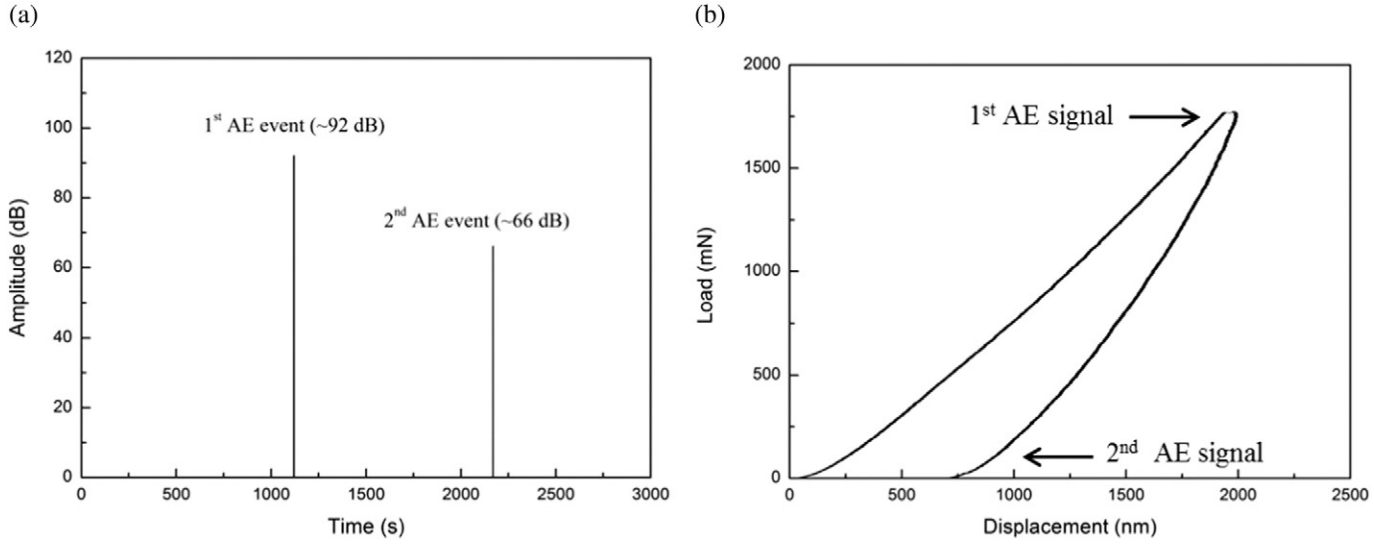


**Fig. 9.** (a) Time history graph and (b) the *P-d* curve of a particular indent on the Cu/Ti/$SiO_2$/Si sample.

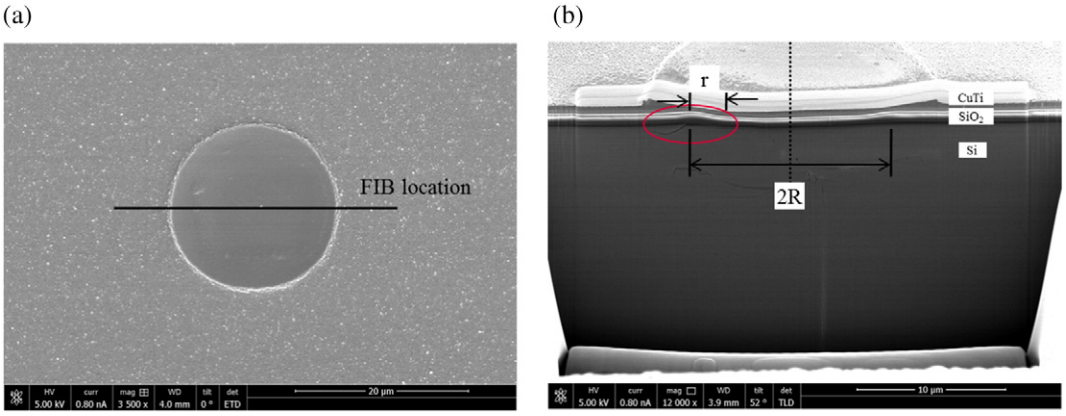


**Fig. 10.** SEM imaging: (a) the top view of the indent and (b) the cross-sectional view of the indented region after FIB cut.

partial delamination, leading to the 'pull off' phenomenon, as shown in Fig. 11. This model is similar to that of the delamination failure mode observed in this indentation damage test whereby part of the circular imprinted area remains adhered to the substrate while delamination occurs at a certain distance away from the center of the indentation.

In this proposed model, an external upward force is applied quasistatically to the cylindrical indenter onto a thin circular film fixed at its circumference, to separate and drive delamination at the indenter-film interface. The thin film has the properties of an elastic modulus $E$, Poisson's ratio $v$, thickness $t$ and radius $R$. When the system reaches equilibrium, the contact area will reduce from initial radius $R$ to $(R\text{-}r)$ and an opening crack displacement $c$ can be obtained (Fig. 11). Based on the energy balance approach, the total energy of the system during the unloading process can be defined as,

$$U = W_c + W_m + W_f \tag{3}$$

where $W_c = A.G$ is the work done to create the interfacial annular crack of area $A = 2\pi r(R-r)$; $W_m = Fc$ is the mechanical work done by the indenter load $F$ and $W_f$ is the stored elastic energy of the annular membrane which is given by:

$$W_f = \frac{4\pi E' t}{(1-\zeta)\log\zeta\log\zeta}\left(\frac{c^4}{4}\right). \tag{4}$$

where $\zeta = \left(\frac{R-r}{R}\right)^2$ and $E' = \frac{E}{1-v}$.

During delamination, the prestress is not released due to the constraints at the circumference. A quasistatic equilibrium is then achieved when $\frac{dU}{dA} = 0$, and from the differential energy balance of Eq. (3), the $G$ can be expressed as:

$$G = \frac{3(2-2\zeta-\zeta\log\zeta)}{\zeta(1-\zeta)^2[\log(1/\zeta]^3}\left(\frac{E' tc^4}{R^4}\right). \tag{5}$$

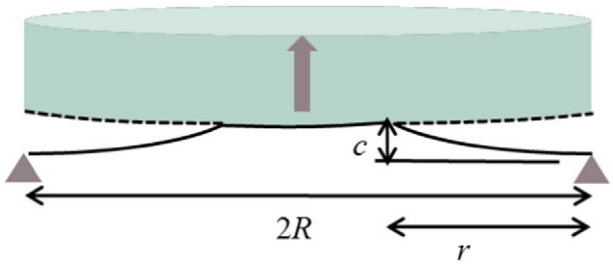


**Fig. 11.** Schematic diagram of the adherence between the flat cylindrical punch and a thin circular film fixed at its perimeter.

Henceforth, the $G$ is calculated to be ~9.79 J/m$^2$ which is slightly larger than ~8.23 J/m$^2$ that is previously obtained by the FEM simulation. This slight overestimation is most likely attributed by the error from the estimation of the crack area which may not be perfectly annular and the presence of residual stress in the real thin-film stack. Nevertheless, the experimental and simulation results are in good agreement.

## 4. Conclusions

A direct and effective combined approach based on MD and CZM-FEM simulations is adopted to characterize the interfacial energies and predict delamination in the Cu/Ti/$SiO_2$/Si multi-layered system. In the approach, the MD simulation is first conducted to obtain the properties of each interface in the Cu/Ti/$SiO_2$/Si multi-layered system. Subsequently, the FEM model is built to simulate the indentation damage of the Cu/Ti/$SiO_2$/Si multi-layered system. The material parameters that are required to be input into the CZM constitutive relation are derived from MD simulation rather than experiment. The thermodynamic work of adhesion is used as the failure criterion for the FEM simulation as it is independent of the system geometry and applied strain rate. During the indentation loading, interfacial delamination occurs at the $SiO_2$/Si interface and the interfacial fracture energy obtained is about 8.23 J/m$^2$.

Lastly, the microindentation experiment is performed on the Cu/Ti/$SiO_2$/Si multi-layered sample to provide validation to the simulation results. During the indentation loading, the high contact stresses results in localized substrate cracking. When the system undergoes the unloading process and the layers undergo different elastic recovery. Such difference causes one of the substrate cracks to propagate towards the weak $SiO_2$/Si interface boundary, resulting in high stress concentration at the $SiO_2$/Si interface. Eventually, interfacial delamination occurs at the $SiO_2$/Si interface which is consistent with the simulation results. The interfacial fracture energy obtained from the indentation damage experiment is about 9.79 J/m$^2$ which is close to that obtained by MD-FEM simulations.

The good agreement between the simulation and experimental results indicates that the approach developed in this work is accurate and effective for obtaining the interfacial properties of multi-layered material systems at the nano- and micro-scale which is very challenging and costly for experimental approaches. The simulation results can be further improved by considering the effect of substrate cracks via the extended-FEM so that a closer modeling of the real failure state can be achieved. Experimentally, the residual stresses of the thin films can also be taken into account to obtain more realistic interfacial fracture energy. Henceforth, this current approach can be utilized to predict interfacial delamination in 3D ICs packaging under different operating conditions, such as the thermal reflow process, thereby improving the reliability of such devices.

## Acknowledgements

This work was supported by Ministry of Education, Singapore (Academic Research Fund TIER 1-RG128/14) and by Economic Development Board of Singapore and Infineon Technologies Asia Pacific Pte Ltd. through the Industrial Postgraduate Programme, Nanyang Technological University, Singapore.

## References

[1] W.R. Davis, J. Wilson, S. Mick, J. Xu, H. Hao, C. Mineo, A.M. Sule, M. Steer, P.D. Franzon, Demystifying 3D ICs: The pros and cons of going vertical, IEEE Des. Test. Comput. 22 (6) (2005) 498–510.
[2] P. Lin, R.I. Babicheva, M. Xue, H.S. Zhang, H. Xu, B. Liu, K. Zhou, Effects of temperature and voids on the interfacial fracture of Si/a-$Si_3N_4$ bilayer systems, Phys. Status Solidi B 252 (9) (2015) 2013–2019.
[3] M. Kriese, N. Moody, W. Gerberich, Effects of annealing and interlayers on the adhesion energy of copper thin films to $SiO_2$/Si substrates, Acta Mater. 46 (18) (1998) 6623–6630.
[4] L. Zhang, P. Yang, M. Chen, N. Liao, Numerical investigation on thermal properties at Cu–Al interface in micro/nano manufacturing, Appl. Surf. Sci. 258 (8) (2012) 3975–3979.
[5] J. Sanchez, S. El-Mansy, B. Sun, T. Scherban, N. Fang, D. Pantuso, W. Ford, M. Elizalde, J. Martınez-Esnaola, A. Martın-Meizoso, Cross-sectional nanoindentation: a new technique for thin film interfacial adhesion characterization, Acta Mater. 47 (17) (1999) 4405–4413.
[6] D.B. Marshall, A.G. Evans, Failure mechanisms in ceramic-fiber/ceramic-matrix composites, J. Am. Ceram. Soc. 68 (5) (1985) 225–231.
[7] A. Volinsky, N. Moody, W. Gerberich, Interfacial toughness measurements for thin films on substrates, Acta Mater. 50 (3) (2002) 441–466.
[8] M.P. Hughey, D.J. Morris, R.F. Cook, S.P. Bozeman, B.L. Kelly, S.L. Chakravarty, D.P. Harkens, L.C. Stearns, Four-point bend adhesion measurements of copper and permalloy systems, Eng. Fract. Mech. 71 (2) (2004) 245–261.
[9] L.R. Katipelli, A. Agarwal, N.B. Dahotre, Interfacial strength of laser surface engineered TiC coating on 6061 Al using four-point bend test, Mater. Sci. Eng. A 289 (1) (2000) 34–40.
[10] S.S.V. Kandula, C.D. Hartfield, P.H. Geubelle, N.R. Sottos, Adhesion strength measurement of polymer dielectric interfaces using laser spallation technique, Thin Solid Films 516 (21) (2008) 7627–7635.
[11] J. Vossen, Measurements of film-substrate bond strength by laser spallation, Adhesion Measurement of Thin Films, Thick Films, and Bulk Coatings, ASTM International, 1978.
[12] M. Ortiz, A. Pandolfi, Finite-deformation irreversible cohesive elements for three-dimensional crack-propagation analysis, Int. J. Numer. Meth. Eng. 44 (1999) 1267–1282.
[13] M. Lu, H. Huang, Determination of the energy release rate in the interfacial delamination of silicon nitride film on gallium arsenide substrate via nanoindentation, J. Mater. Res. 29 (06) (2014) 801–810.
[14] P. Lin, C.M. Chai, M. Xue, H. Xu, K. Zhou, An approach for the prediction of interfacial delamination of a-$Si_3N_4$/Si bilayer system, J. Phys. D. Appl. Phys. (2016) (in press).
[15] S. Namilae, N. Chandra, Multiscale model to study the effect of interfaces in carbon nanotube-based composites, J. Eng. Mater. Technol. ASME 127 (2) (2005) 222–232.
[16] H.B. Fan, M.M.F. Yuen, A multi-scale approach for investigation of interfacial delamination in electronic packages, Microelectron. Reliab. 50 (7) (2010) 893–899.
[17] M. De Boer, W. Gerberich, Microwedge indentation of the thin film fine line—I. Mechanics, Acta Mater. 44 (8) (1996) 3169–3175.
[18] M. De Boer, W. Gerberich, Microwedge indentation of the thin film fine line—II. Experiment, Acta Mater. 44 (8) (1996) 3177–3187.
[19] S. Zhang, X. Zhang, Toughness evaluation of hard coatings and thin films, Thin Solid Films 520 (7) (2012) 2375–2389.
[20] H. Fan, M. Yuen, A multiscale approach for interfacial delamination in solid-state lighting, Solid State Lighting Reliability, Springer 2013, pp. 305–316.
[21] S. Shen, S. Atluri, Atomic-level stress calculation and continuum-molecular system equivalence, Comput. Model. Eng. Sci. 6 (2004) 91–104.
[22] B. Wang, X. Sun, Q. Fan, Y. Yin, Numerical simulation of interfacial delamination in electronic packaging, Thermal and Thermomechanical Phenomena in Electronic Systems ITHERM 2000, Intersoc. C. Thermal. T. IEEE, 2000.
[23] G. Tanaka, L.A. Goettler, Predicting the binding energy for nylon 6, 6/clay nanocomposites by molecular modeling, Polymer 43 (2) (2002) 541–553.
[24] F.F. Abraham, H. Gao, How fast can cracks propagate? Phys. Rev. Lett. 84 (14) (2000).
[25] E. Gerde, M. Marder, Friction and fracture, Nature 413 (6853) (2001) 285–288.
[26] M. Cordill, N. Moody, D. Bahr, Quantifying improvements in adhesion of platinum films on brittle substrates, J. Mater. Res. 19 (6) (2004) 1818–1825.
[27] S.R. Billeter, A. Curioni, D. Fischer, W. Andreoni, *Ab initio* derived augmented Tersoff potential for silicon oxynitride compounds and their interfaces with silicon, Phys. Rev. B 73 (15) (2006) 155329.
[28] M. Baskes, R. Johnson, Modified embedded atom potentials for HCP metals, Model. Simul. Mater. Sci. Eng. 2 (1) (1994) 147.
[29] M. Baskes, Application of the embedded-atom method to covalent materials: a semiempirical potential for silicon, Phys. Rev. Lett. 59 (23) (1987) 2666.
[30] S. Plimpton, Fast parallel algorithms for short-range molecular dynamics, J. Comput. Phys. 117 (1) (1995) 1–19.
[31] A. Ural, V.R. Krishnan, K.D. Papoulia, A cohesive zone model for fatigue crack growth allowing for crack retardation, Int. J. Solids S. Struct. 46 (11) (2009) 2453–2462.
[32] V. Yamakov, E. Saether, D.R. Phillips, E.H. Glaessgen, Molecular-dynamics simulation-based cohesive zone representation of intergranular fracture processes in aluminum, J. Mech. Phys. Solids 54 (9) (2006) 1899–1928.
[33] W.-P. Wu, N.-L. Li, Y.-L. Li, Molecular dynamics-based cohesive zone representation of microstructure and stress evolutions of nickel intergranular fracture process: effects of temperature, Comp. Mater. Sci. 113 (2016) 203–210.
[34] C. Shet, N. Chandra, Analysis of energy balance when using cohesive zone models to simulate fracture processes, J. Eng. Mater. Technol. ASME 124 (4) (2002) 440–450.
[35] T.-H. Fang, W.-J. Chang, Nanomechanical properties of copper thin films on different substrates using the nanoindentation technique, Microelectron. Eng. 65 (2003) 231–238.
[36] W.C. Oliver, G.M. Pharr, Measurement of hardness and elastic modulus by instrumented indentation: advances in understanding and refinements to methodology, J. Mater. Res. 19 (2004) 1–20.
[37] S. Nemat-Nasser, W.G. Guo, J.Y. Cheng, Mechanical properties and deformation mechanisms of a commercially pure titanium, Acta Mater. 47 (1999) 3705–3720.
[38] A. Needleman, A continuum model for void nucleation by inclusion debonding, J. Appl. Phys. 54 (3) (1987) 525–531.
[39] S. Igor, L. Cizelj, Cohesive zone modeling of intergranular cracking in polycrystalline aggregates, Nucl. Eng. Des. 283 (2015) 139–147.
[40] K. Nagao, J. Neaton, N. Ashcroft, First-principles study of adhesion at Cu/$SiO_2$ interface, Phys. Rev. B 68 (12) (2003) 125403.
[41] A. Furuya, Y. Ohshita, Ti concentration effect on adhesive energy at Cu/TiW interface, J. Appl. Phys. 84 (9) (1998) 4941–4944.
[42] D. Li, F. Wang, Z. Yang, Y. Zhao, How to identify dislocations in molecular dynamics simulations? Sci. China Phys. Mech. Astron. 57 (12) (2014) 2177–2187.
[43] K.-T. Wan, D.A. Dillard, Adhesion of a flat punch adhered to a thin pre-stressed membrane, J. Adhes. 79 (2) (2003) 123–140.